

Synthesis of ¹⁹F Nucleic Acid–Polymer Conjugates as Real-Time MRI Probes of Biorecognition

Giovanna Sicilia,^{*a} Adrienne L. Davis,^b Sebastian G. Spain,^c Johannes P. Magnusson,^a Nathan R.B. Boase,^{d,e} Kristofer J. Thurecht,^{*d,e} and Cameron Alexander.^{*a}

^a School of Pharmacy and ^b School of Chemistry, University of Nottingham, University Park, Nottingham, NG7 2RD. UK.

^c School of Chemistry, University of Sheffield, Sheffield, S3 7HF.

^d Australian Institute for Bioengineering and Nanotechnology and ^e Centre for Advanced Imaging, The University of Queensland, St Lucia, Queensland, 4072, Australia.

Analytical methods.....	2
High performance liquid chromatography (HPLC).....	2
Matrix-assisted laser desorption/ionization time-of-flight mass spectrometry (MALDI-TOF).....	2
Native Polyacrylamide gel electrophoresis (PAGE).....	2
Gel Permeation Chromatography (GPC) of p(MAm-c-MAmA1).....	2
Dynamic light scattering (DLS) of p(MAm-c-MAmA1).....	2
Buffers and solutions.....	3
Lists of relaxation delays, echo and recovery times.....	4
¹ H and ¹⁹ F T_2 , T_1 curve fitting.....	5
¹ H and ¹⁹ F T_2 , T_1 diffusion curve fitting.....	6
MALDI and HPLC analysis of oligonucleotides.....	6
PAGE analysis of oligonucleotides.....	7
¹ H T_2 and T_1 relaxation of oligonucleotideB2.....	8
¹ H and ¹⁹ F diffusion analysis of oligonucleotide B2.....	9
Synthesis and characterisation of p(MAm-c-MAmA1).....	10
Calculation of p(MAm-c-MAmA1) composition.....	12
¹ H T_2 and T_1 relaxation of p(MAm-c-MAmA1).....	14
¹ H diffusion analysis of p(MAm-c-MAmA1).....	15
PAGE analysis of p(MAm-c-MAmA1B2).....	16
¹ H T_2 and T_1 relaxation of p(MAm-c-MAmA1B2).....	17
¹ H diffusion analysis of p(MAm-c-MAmA1B2).....	18
¹⁹ F diffusion analysis of B2, p(MAm-c-MAmA1B2) and p(MAm-c-MAmA1B2)+C.....	19
PAGE analysis of p(MAm-c-MAmA1B2)C.....	19
¹ H T_2 and T_1 relaxation of p(MAm-c-MAmA1B2)C.....	20
¹ H diffusion analysis of p(MAm-c-MAmA1B2)C.....	21

Analytical methods

High performance liquid chromatography (HPLC)

High performance liquid chromatography (HPLC) was performed on a Shimadzu Prominence UPLC system fitted with a DGU-20A5 degasser, LC-20AD low pressure gradient pump, CBM-20A LITE system controller, SIL-20A autosampler and an SPD-M20A diode array detector.

Ion exchange HPLC (IE-HPLC) analytical and semi-preparative separations were performed on a Dionex DNAPac PA 100 anion exchange column (13.5 μm , 9 \times 250 mm) with a convex gradient of 100 to 450 mM NaCl in the presence of 0.25 M Tris·HCl, pH 8.0 at a flow rate of 5.0 mL min⁻¹.

Reverse phase HPLC (rp-HPLC) analytical separations were performed on a Phenomenex Clarity 3 μm Oligo-RP C18 column (4.6 \times 50mm) with a linear gradient of 5 - 30% acetonitrile (ACN) in 0.1 M triethylammonium acetate (TEAA, pH 7.0) at a flow rate of 1 mL min⁻¹ as a mobile phase.

Matrix-assisted laser desorption/ionization time-of-flight mass spectrometry (MALDI-TOF)

Matrix-assisted laser desorption/ionization time-of-flight (MALDI-TOF) mass spectrometry was performed on a Bruker MALDI-TOF Ultraflex III spectrometer operated in linear, positive ion mode with a N₂ laser of 337 nm and pulses of 3 ns. Samples were prepared with 3-hydroxypicolinic acid in ammonium citrate dibasic as a matrix solution. Specifically, a saturated solution of 3-HPA (50 mg/mL) was prepared by adding 25 mg of 3-HPA to 500 μL of water and vortexing for 1 min; a sediment remained at the bottom of the tube after this step. Ammonium citrate dibasic solution (25 μL of 50 mg/ml) was added to saturated 3-HPA solution (225 μL). Equal volumes of matrix solution and analyte solution (0.2 mM) were mixed and 2 μL of the mixture was spotted onto the MALDI plate and allowed to evaporate.

Native Polyacrylamide gel electrophoresis (PAGE)

Preparation of samples. Samples were prepared by dilution in annealing buffer (Table S1). 1 μL of 10% (w/v) glycerol was added to each sample. Loading dye (Orange G) was added only to the ladder.

Preparation of gels. Gel casting solution was prepared by mixing the components described in Table S1† and carefully pipetted into preassembled plate. A 10 well comb was inserted and the gel allowed setting for 40 min.

Electrophoresis. Gels were pre-run for 20 minutes at 200V in 1 \times TBE. Samples were loaded at approximately 200 pmoles per well. Gels were run until the Orange G loading dye migrated out from the gel (approximately 180 min).

Staining. Gels were washed with water then stained with 0.1% (w/v) methylene blue in 0.5 M sodium acetate pH 5.2 for 30 min. Excess staining was removed by destaining with distilled water until the bands were clear against the background. Images were recorded using a standard flatbed scanner (HP Scanjet 2710).

Gel Permeation Chromatography (GPC) of p(MAm-c-MAmA1)

Aqueous GPC was performed on a Shimadzu Prominence UPLC fitted with differential refractive index (RI) detector. The eluent was Dulbecco's PBS without Ca²⁺ and Mg²⁺ at 35°C and a flow rate of 1 mL·min⁻¹. The instrument was fitted with a Polymer Labs aquagel-OH guard column (50 \times 7.5 mm, 8 μm) followed by three PL aquagel-OH columns (30, 40 and 50; 300 \times 7.5 mm, 8 μm). Column calibration was achieved using narrow PEG/PEO standards of known M_p in the range of 200 Da – 130 kDa. Molecular weights and dispersity values were calculated using Shimadzu LabSolutions software with GPC analysis add-on. p(MAm-c-MAmA1) was dissolved in water BPC grade at a concentration of 4 mg/mL.

Dynamic light scattering (DLS) of p(MAm-c-MAmA1)

Dynamic light-scattering was performed on a Viscotek 802 DLS instrument fitted with an internal laser (λ 830 \pm 5 nm, Pmax 60 mW). p(MAm-c-MAmA1) (0.5 mg/mL in water BPC grade) was analysed before

and after filtration through a 4 mm syringe filter PVDF 0.2 μ m membrane. Laser power was adjusted to until detection rate of at least 300 kcps was achieved. A series of 10 \times 3 seconds experiments was recorded and hydrodynamic radii distributions calculated with Viscotek OmniSize3 software.

Buffers and solutions

Table S1 Buffers and solution used for PAGE analysis.

Solution	Components
Annealing Buffer	10 mM Tris pH 7.5/ 50mM NaCl/ 1mM EDTA Dissolved in DNase free water and adjusted to pH 7.5
Loading dye solution	100 μ L glycerol 100 μ L 10 \times TBE 20 μ L 7.5% Orange G 780 μ L H ₂ O
Native PAGE gel 30%	5.6 mL 40% acrylamide-bis-acrylamide 29/1 1.5 mL 10 \times TBE 0.4 mL H ₂ O To this solution 10% APS (75 μ L) and TEMED (7.5 μ L) were added to initiate the polymerization
Native PAGE gel 20%	3.7 mL 40% acrylamide-bis-acrylamide 29/1 1.5 mL 10 \times TBE 0.4 mL H ₂ O To this solution 10% APS (75 μ L) and TEMED (7.5 μ L) were added to initiate the polymerization
Methylene blue staining solution	0.2 g methylene blue 13.61 g sodium acetate 200 mL H ₂ O The solution was adjusted to pH 5.2

Lists of relaxation delays, echo and recovery times

In all ^1H and ^{19}F relaxation experiments delays were randomised in the list to reduce the occurrence of systematic errors.

Table S2 List of relaxation delays and echo times used in ^1H T_2 measurements.

Sample ID	Relaxation Delay (s)	Echo Times (ms)
^{19}F -B2	10	2, 6, 10, 12, 14, 24, 40, 80, 150, 200, 360, 500
p(MAm-c-MAmA1)	15	2, 4, 6, 8, 10, 12, 14, 18, 20, 24, 40, 60, 150, 200, 360, 500
p(MAm-c-MAmA1B2)	10	2, 6, 10, 12, 14, 24, 40, 80, 150, 200, 360, 500
p(MAm-c-MAmA1B2) + C	10	2, 6, 10, 12, 14, 24, 40, 80, 150, 200, 360, 500

Table S3 List of relaxation delays and recovery times used in ^1H T_1 measurements.

Sample ID	Relaxation Delay (s)	Recovery Times (ms)
^{19}F -B2	12	4, 30, 120, 300, 500, 1200, 1600, 2500, 8000, 12000
p(MAm-c-MAmA1)	16	4, 30, 80, 120, 300, 360, 500, 1200, 1600, 2500, 10000, 18000
p(MAm-c-MAmA1B2)	12	4, 30, 120, 300, 500, 1200, 1600, 2500, 8000, 12000
p(MAm-c-MAmA1B2) + C	12	4, 30, 120, 300, 500, 1200, 1600, 2500, 8000, 12000

Table S4 List of relaxation delays and echo times used in ^{19}F T_2 measurements.

Sample	Relaxation Delay (s)	Echo Times (ms)
^{19}F -B2	4	2, 4, 6, 8, 10, 12, 14, 16, 18, 20, 22, 24, 30, 36
p(MAm-c-MAmA1B2)	3	2, 4, 6, 8, 10, 14, 18, 24
p(MAm-c-MAmA1B2) + C	3	2, 4, 6, 8, 10, 12, 14, 18, 20, 24

Table S5 List of relaxation delays and recovery times of ^{19}F T_1 measurements.

Sample	Relaxation Delay (s)	Recovery Times (ms)
^{19}F -B2	5	4, 30, 80, 100, 200, 300, 360, 400, 500, 800, 1000, 1200, 1600, 2500, 4050, 5000
p(MAm-c-MAmA1B2)	2.5	4, 30, 80, 100, 300, 360, 600, 1200, 2500
p(MAm-c-MAmA1B2) + C	2.5	4, 30, 80, 100, 150, 300, 360, 500, 600, 1200, 2000, 2500

 ^1H and ^{19}F T_2 , T_1 curve fitting**Table S6** Exponential decay equations calculated by SigmaPlot 10.0.

Function	Equation	Variables & Coefficients
Single exponential		
2 parameters	$y = ae^{-bx}$	$y = I_\tau; x = \tau; b = \frac{1}{T_1} \text{ or } \frac{1}{T_2}$
3 parameters	$y = y_0 + ae^{-bx}$	
Double exponential		
4 parameters	$y = ae^{-bx} + ce^{-dx}$	$a = P; b = \frac{1}{T_1^{\text{Short}}} \text{ or } \frac{1}{T_2^{\text{Short}}}$
5 parameters	$y = y_0 + ae^{-bx} + ce^{-dx}$	$c = (1 - P); d = \frac{1}{T_1^{\text{Long}}} \text{ or } \frac{1}{T_2^{\text{Long}}}$

The coefficients (a, b, c, d, y_0) of the independent variable (x) that gave the best fit between the equation and the data were determined from the SigmaPlot non-linear regression using the Marquardt-Levenberg algorithm.¹

For single exponential decay rates T_1 and T_2 were calculated as follows:

$$T_1 \text{ or } T_2 = \frac{1}{b} \quad \text{Eq. S1}$$

For double exponential decay rates T_1^{short} , T_1^{Long} , T_2^{Short} , T_2^{Long} and P were calculated as follows:

$$T_1^{\text{Short}} \text{ or } T_2^{\text{Short}} = \frac{1}{b} \quad \text{Eq. S2}$$

$$T_1^{\text{Long}} \text{ or } T_2^{\text{Long}} = \frac{1}{d} \quad \text{Eq. S3}$$

$$P = \frac{a/c}{(1 + a/c)} \quad \text{Eq. S4}$$

¹H and ¹⁹F T₂, T₁ diffusion curve fitting

The integrals of selected regions in the 1D ¹H and ¹⁹F spectra were measured at different gradient strengths and fitted to the Equation 5.²

$$A = A_0 e^{-D\gamma^2 g^2 \delta^2 (\Delta - \frac{\delta}{3} - \frac{\tau}{2})} \quad \text{Eq.S5}$$

where A is the measured integral area; A_0 is the integral area at zero gradient strength; D is the diffusion coefficient; γ is the gyromagnetic ratio of the observed nucleus; g is the gradient strength; δ is the length of the gradient; Δ is the diffusion time and τ is the recovery delay between bipolar gradients. By mathematical rearrangement, the Equation 5 was converted into Equation 6.

$$-\ln A = D\gamma^2 g^2 \delta^2 (\Delta - \frac{\delta}{3} - \frac{\tau}{2}) - \ln A_0 \quad \text{Eq. S6}$$

Since D , γ , δ , Δ and τ are constant, they were converted into a new constant D^* as follows:

$$D^* = D\gamma^2 \delta^2 (\Delta - \frac{\delta}{3} - \frac{\tau}{2})$$

By substitution of the new constant D^* , the Equation 6 was transformed into a linear Equation 7

$$-\ln A = D^* g^2 - \ln A_0 \quad \text{Eq. S7}$$

As shown in Equation 7, D^* represents the slope of the line fitting obtained by plotting $-\ln A$ versus the squared gradient (g^2). Therefore, the diffusion coefficient D was calculated as follows:

$$D = \frac{D^*}{\gamma^2 \delta^2 (\Delta - \delta/3 - \tau/2)} \quad \text{Eq. S8}$$

MALDI and HPLC analysis of oligonucleotides

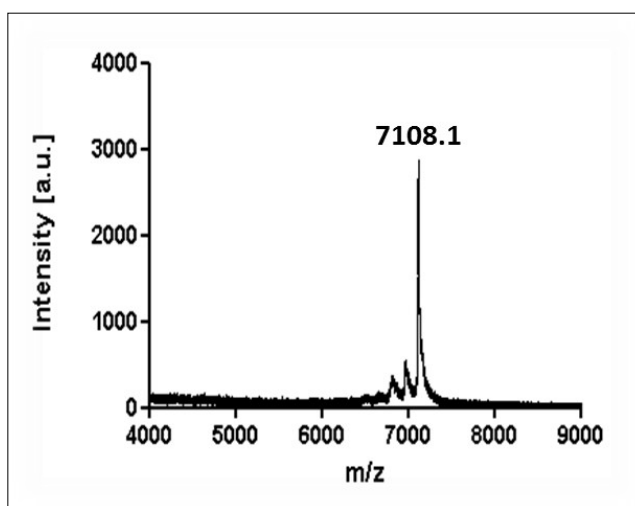


Fig. S1 MALDI-TOF spectrum of 5'-methacrylamidyl oligonucleotide A1 after reverse-phase HPLC purification.

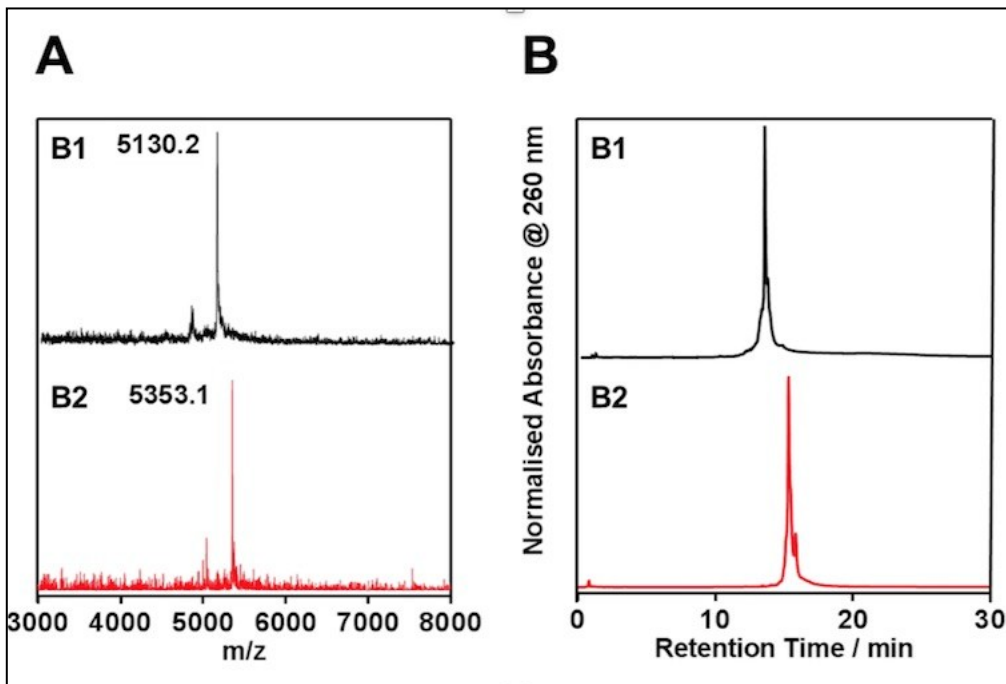


Fig. S2 (A) MALDI-TOF spectra and (B) HPLC chromatograms of 2'-fluoro modified oligonucleotides B1 and B2 after OPC[®] cartridge purification.

PAGE analysis of oligonucleotides

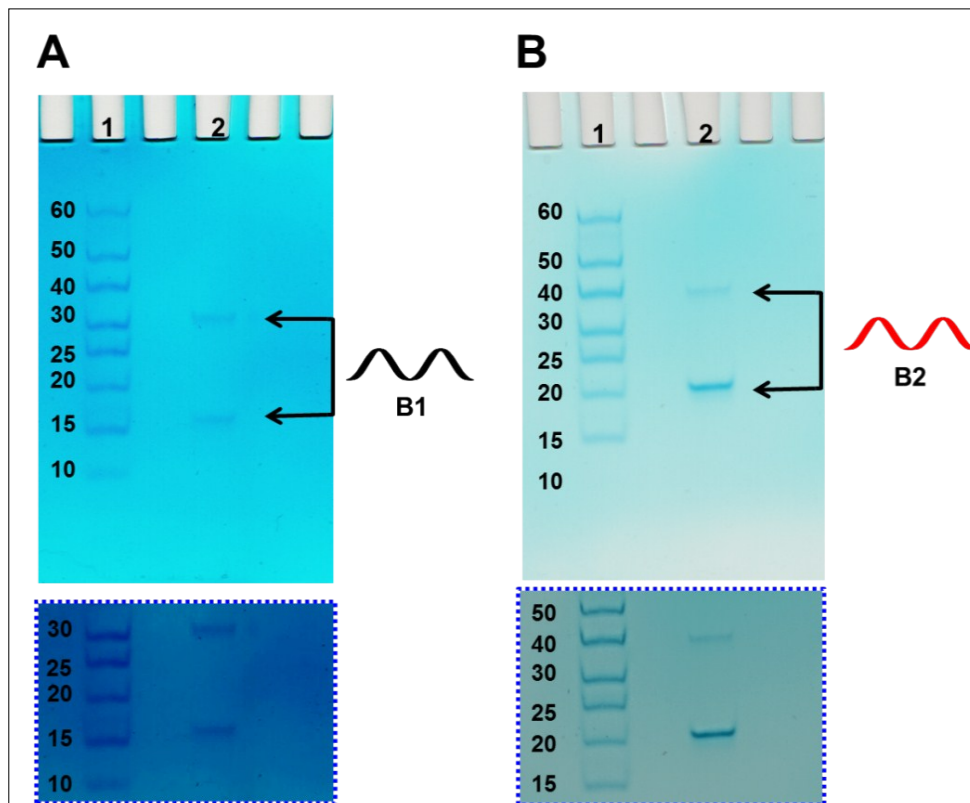


Fig. S3 (A) 30% native PAGE of oligonucleotide B1. Lanes: 1. 10/60 Oligo length standard, 2. B1. (B) 30% native PAGE of oligonucleotide B2. Lanes: 1. 10/60 Oligo length standard, 2. B2. The insets show a selected PAGE section with enhanced contrast.

^1H T_2 and T_1 relaxation of oligonucleotide B2

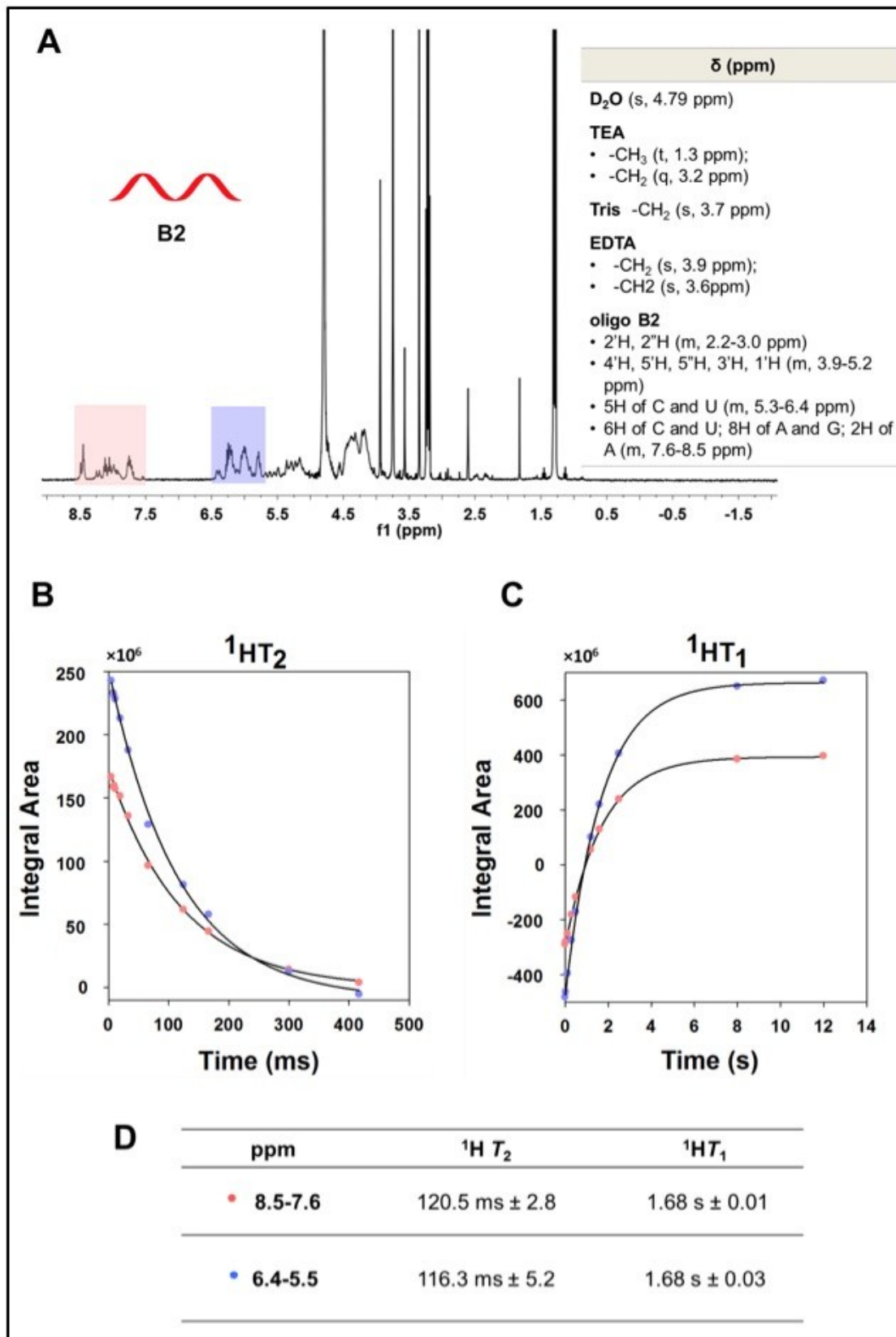


Fig. S4 (A) 1D ^1H NMR of 2'-fluoro modified oligonucleotide B2 in D_2O containing 50 mM NaCl, 10 mM Tris·HCl, 2mM EDTA pH 7.5 with relative ^1H chemical shift assignments. (B) T_2 relaxation time measurements for ^1H resonating at 8.5-7.6 ppm (pink circles) and 6.4-5.5 ppm (blue circles) fitted with single exponential decay curves. (C) T_1 relaxation time measurements for ^1H resonating at 8.5-7.6 ppm (pink circles) and 6.4-5.5 ppm (blue circles) fitted with single exponential decay curves. (D) List of $^1\text{H } T_2$ and T_1 relaxation times measured for protons resonating at 8.5-7.6 ppm and 6.4-5.5 ppm with their relative standard errors.

¹H and ¹⁹F diffusion analysis of oligonucleotide B2

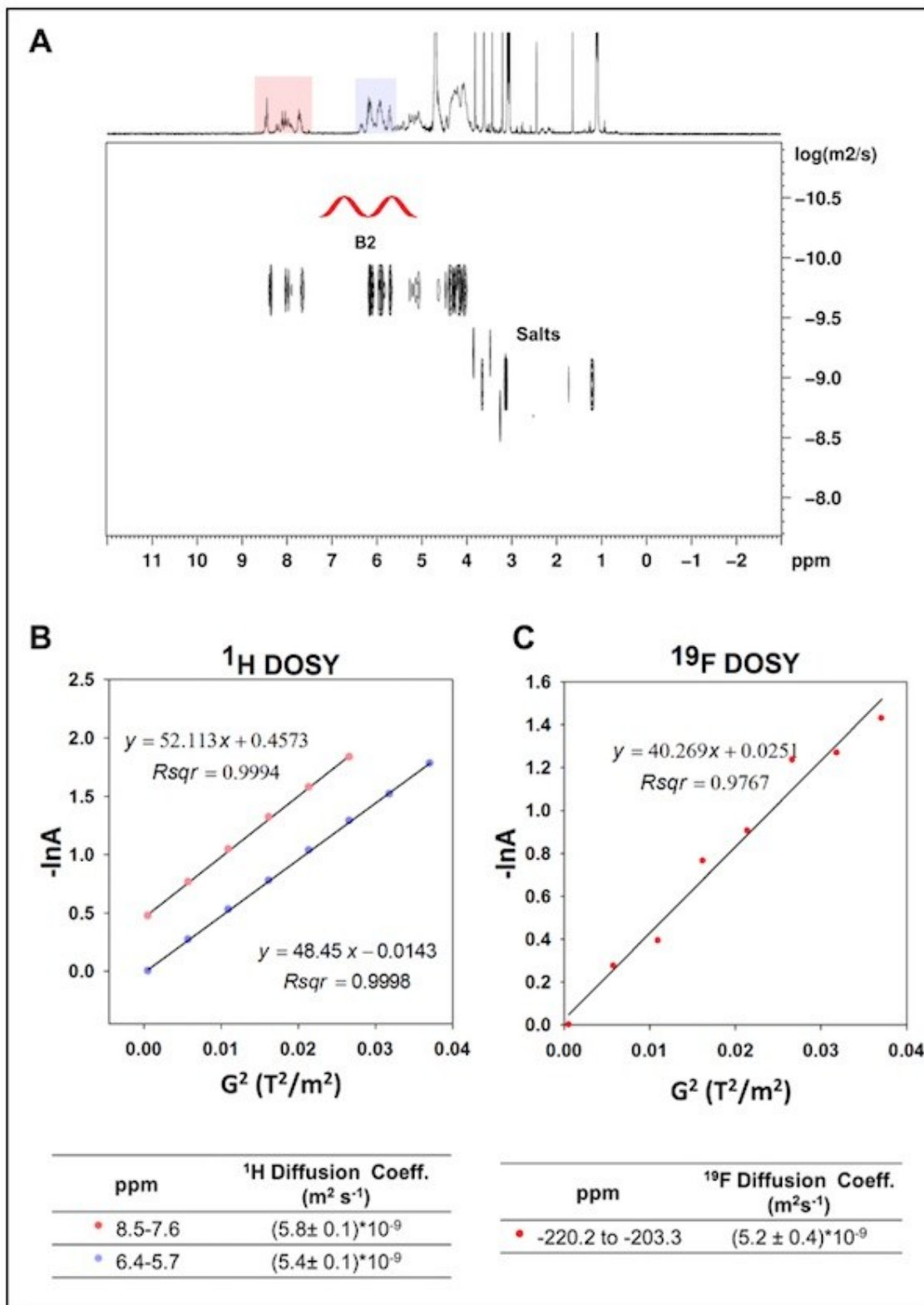


Fig. S5 (A) 2D ¹H DOSY spectrum of oligonucleotide B2. The regions selected for fitting analysis are highlighted in pink and blue in the F2 projection. (B) The negative natural logarithm of the area of selected ¹H peaks resonating at 8.5-7.6 ppm and 6.4-5.7 ppm is plotted against the squared gradient strength. ¹H Diffusion coefficients are listed with their relative standard deviation. (C) The negative natural logarithm of the area of the ¹⁹F signal detected for oligo B2 is plotted against the squared gradient strength. The ¹⁹F self-diffusion coefficient measured for the fluorine spins of oligo B2 is listed with its relative standard deviation.

Synthesis and characterisation of p(MAm-c-MAmA1)

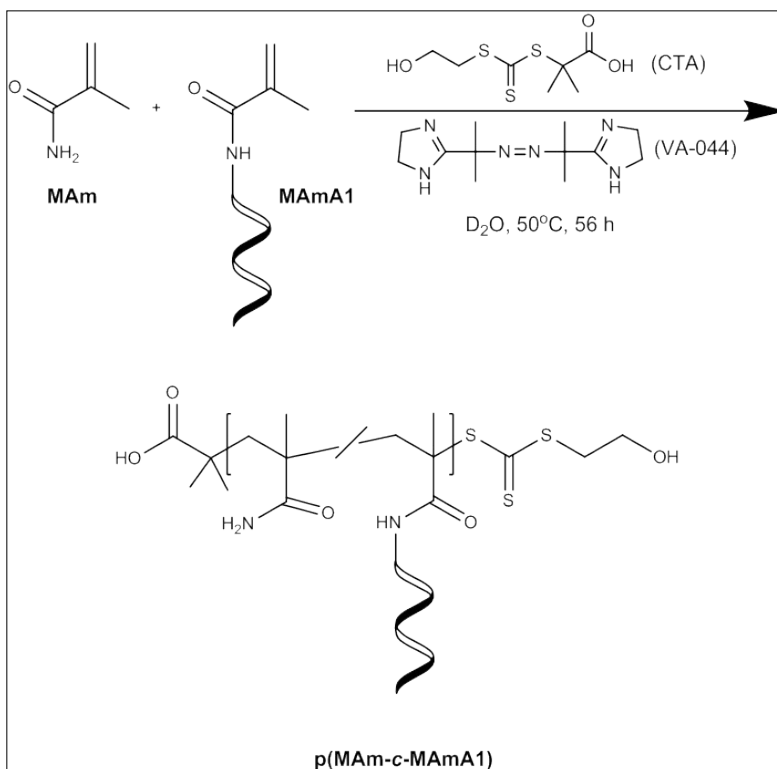


Fig. S6 Synthesis of p(MAm-c-MAmA1) *via* aqueous RAFT polymerization.

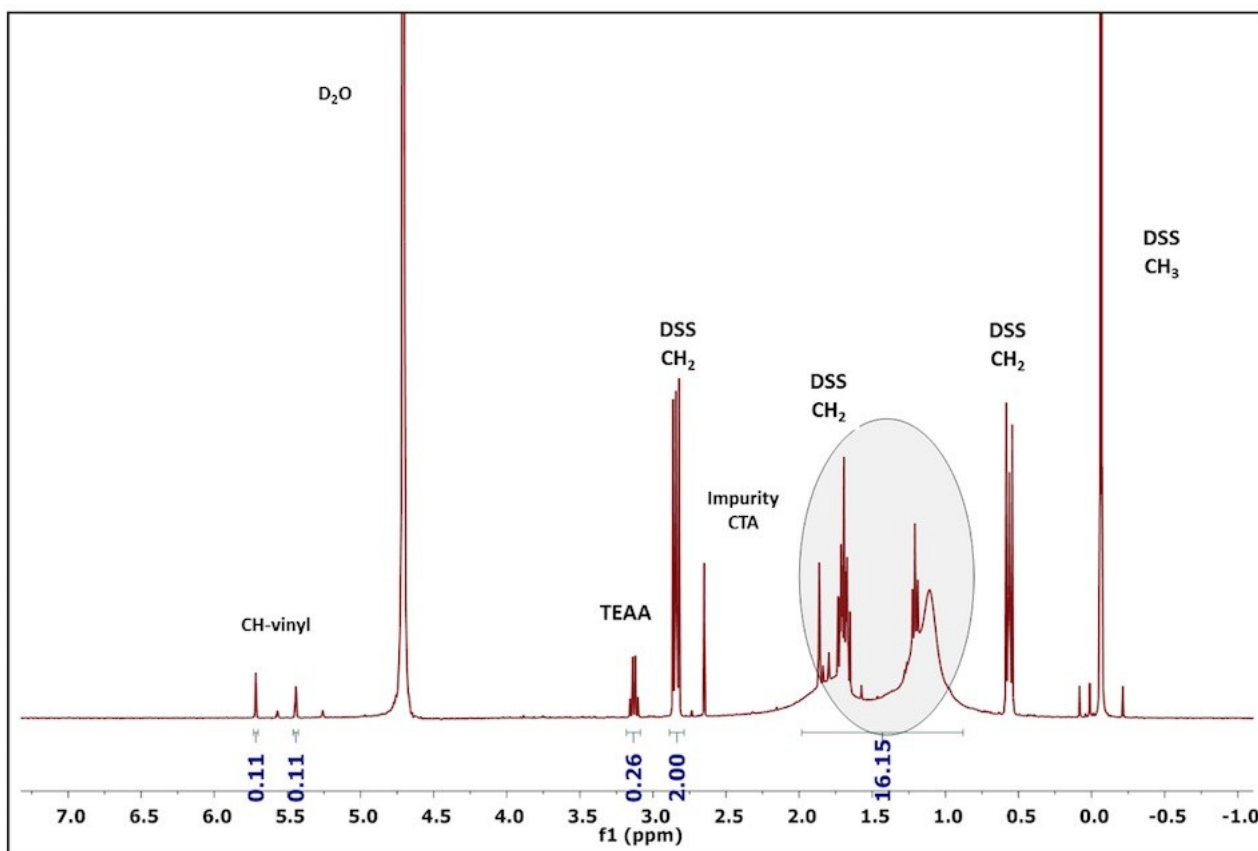


Fig. S7 1D ¹H NMR acquired after solubilisation in D₂O of the gel formed during the synthesis of p(MAm-c-MAmA1). 4,4-dimethyl-4-silapentane-1-sulfonic acid (DSS) was used as internal standard.

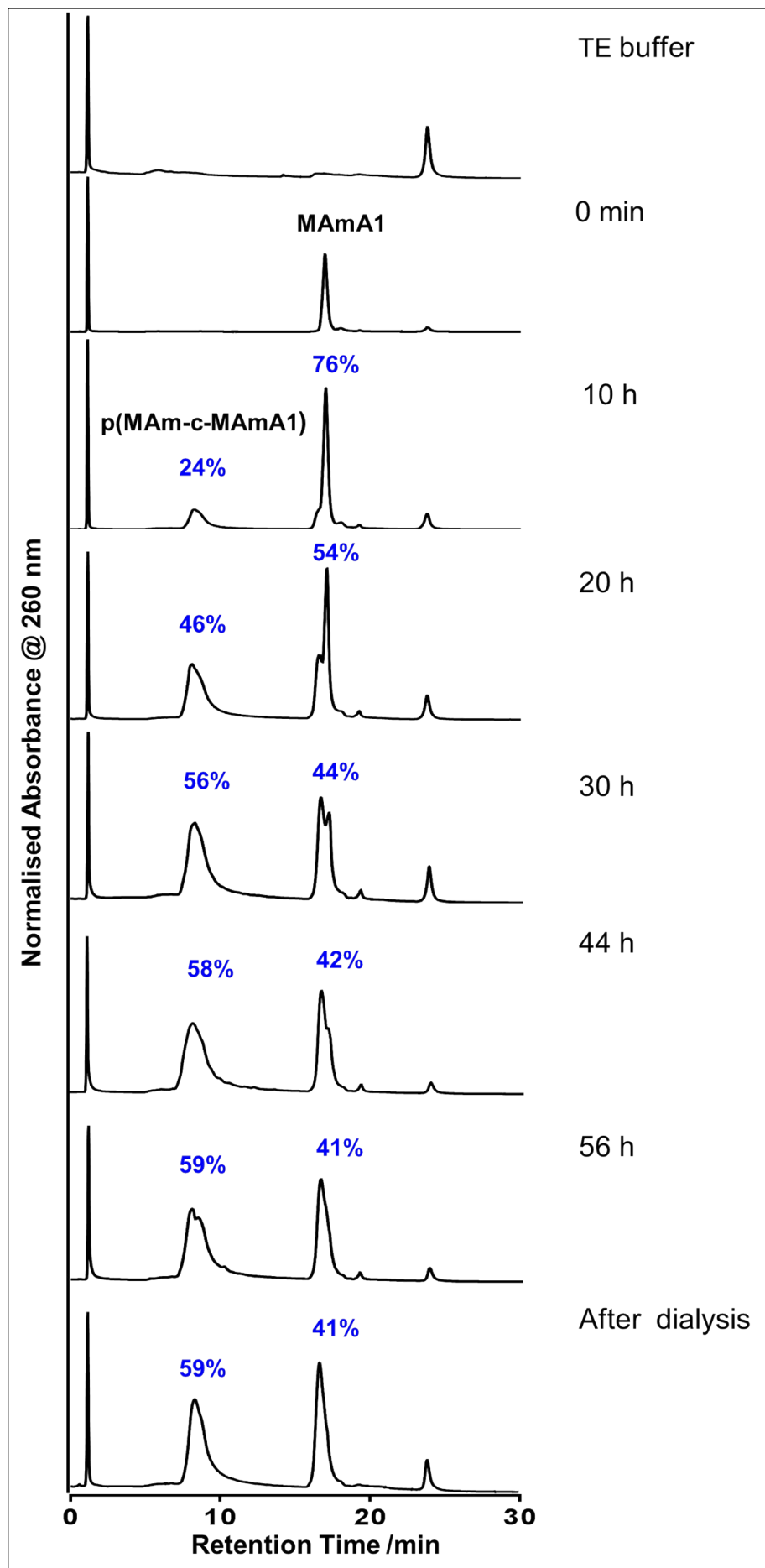


Fig. S8 HPLC chromatograms acquired during the synthesis of p(MAm-c-MAmA1) and after dialysis of the reaction mixture.

Calculation of p(MAm-c-MAmA1) composition

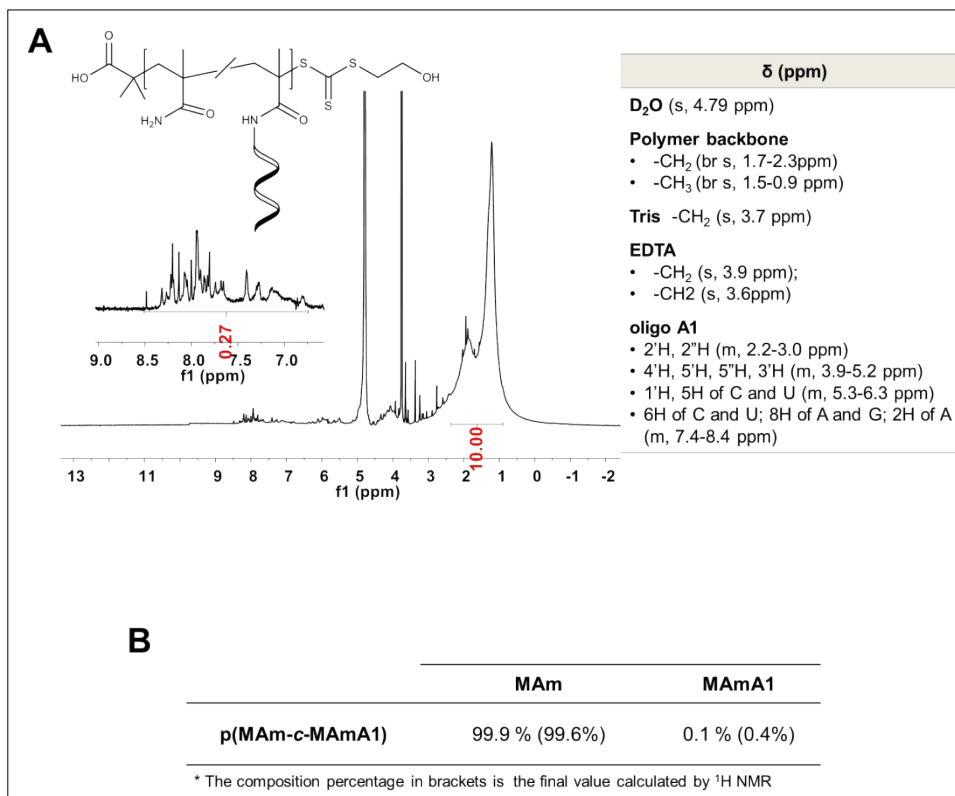


Fig. S9 (A) 1D ¹H NMR spectrum of p(MAm-c-MAMa1) after HPLC purification with relative list of ¹H chemical shift assignments. The sample was dissolved in D₂O containing 50 mM NaCl, 10 mM Tris·HCl, 2 mM EDTA pH 7.5. (B) Composition percentage of the monomer units MAM and MAMa1 constituting p(MAm-c-MAMa1) after HPLC purification.

The final copolymer composition was calculated from the ¹H NMR acquired from the polymer after HPLC purification. As shown in Fig. S8 A, the integrals of MAM and MAMa1 were correlated (Equation S5) employing the protons for MAM (5H, -CH₂ and -CH₃ per monomer unit) and MAMa1 [5H, -CH₂ and -CH₃; 30H, DNA A1 (signals between 8.5-6.9 ppm) per monomer unit] with disregard of the endgroups. The sum of the fractions of MAM (F_x) and MAMa1 (F_y) was set to 100% (Equation S6).

$$\frac{I(-CH_2 - CH_3)}{I(8.5 - 6.9 \text{ ppm})} = \frac{5 \cdot F_x + 5 \cdot F_y}{30 \cdot F_y} \quad \text{Eq. S5}$$

$$F_x + F_y = 1 \quad \text{Eq. S6}$$

The ratio of MAMa1 (F_y) in the copolymer was estimated using Equation S7:

$$\frac{I(-CH_2 - CH_3)}{I(8.5 - 6.9 \text{ ppm})} = \frac{5}{30 \cdot F_y} \quad \text{Eq. S7}$$

Due to relative peak sizes the measurements reported in Figure S9 B should be considered approximate.

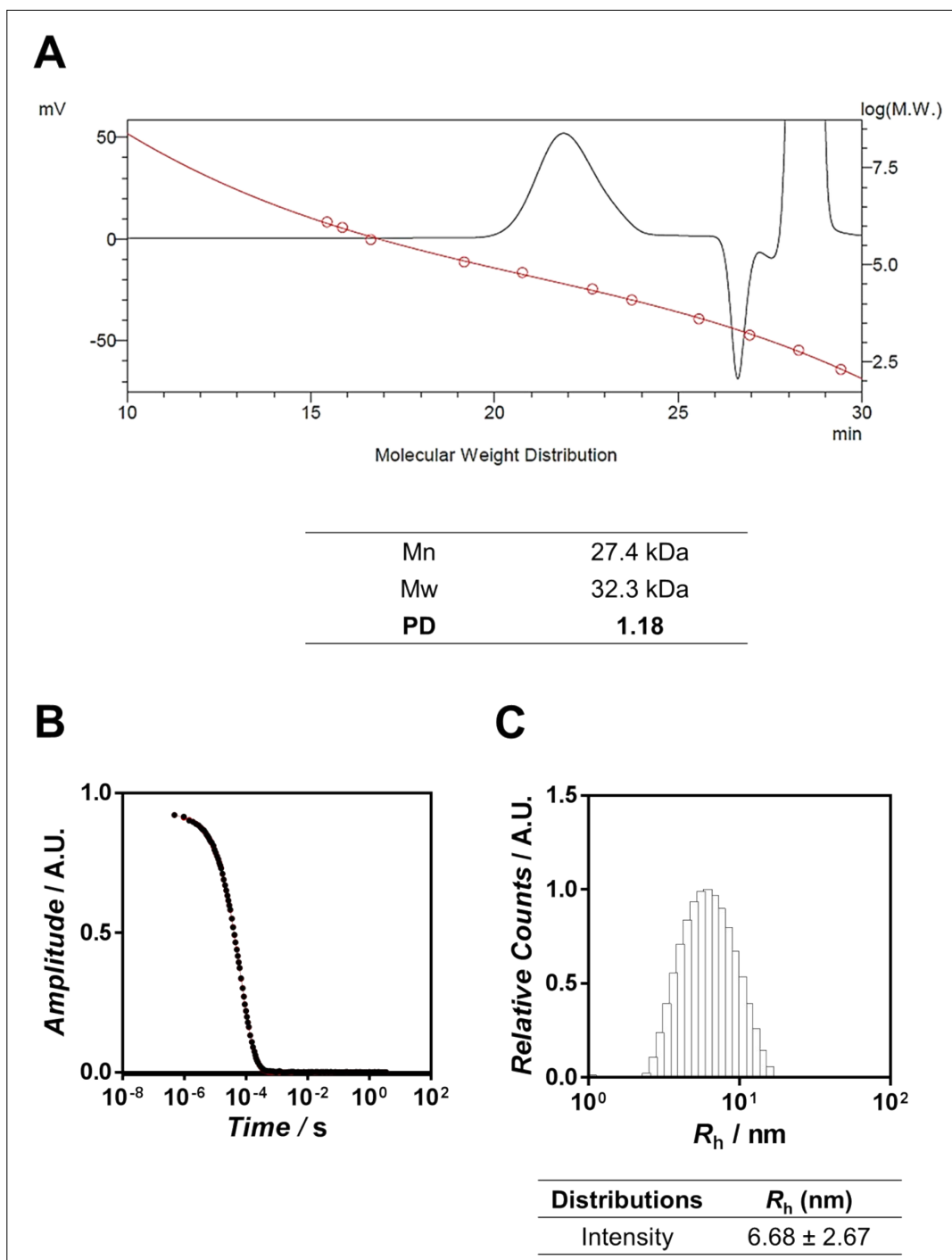


Fig. S10 (A) GPC chromatogram with relative list of M_n , M_w and PD measured for p(MAm-c-MAmA1) after anion exchange HPLC purification. (B) Correlation curve for DLS of p(MAm-c-MAmA1). (C) Dynamic light scattering of p(MAm-c-MAmA1). Intensity distribution with relative list of hydrodynamic radius measured.

^1H T_2 and T_1 relaxation of p(MAm-c-MAmA1)

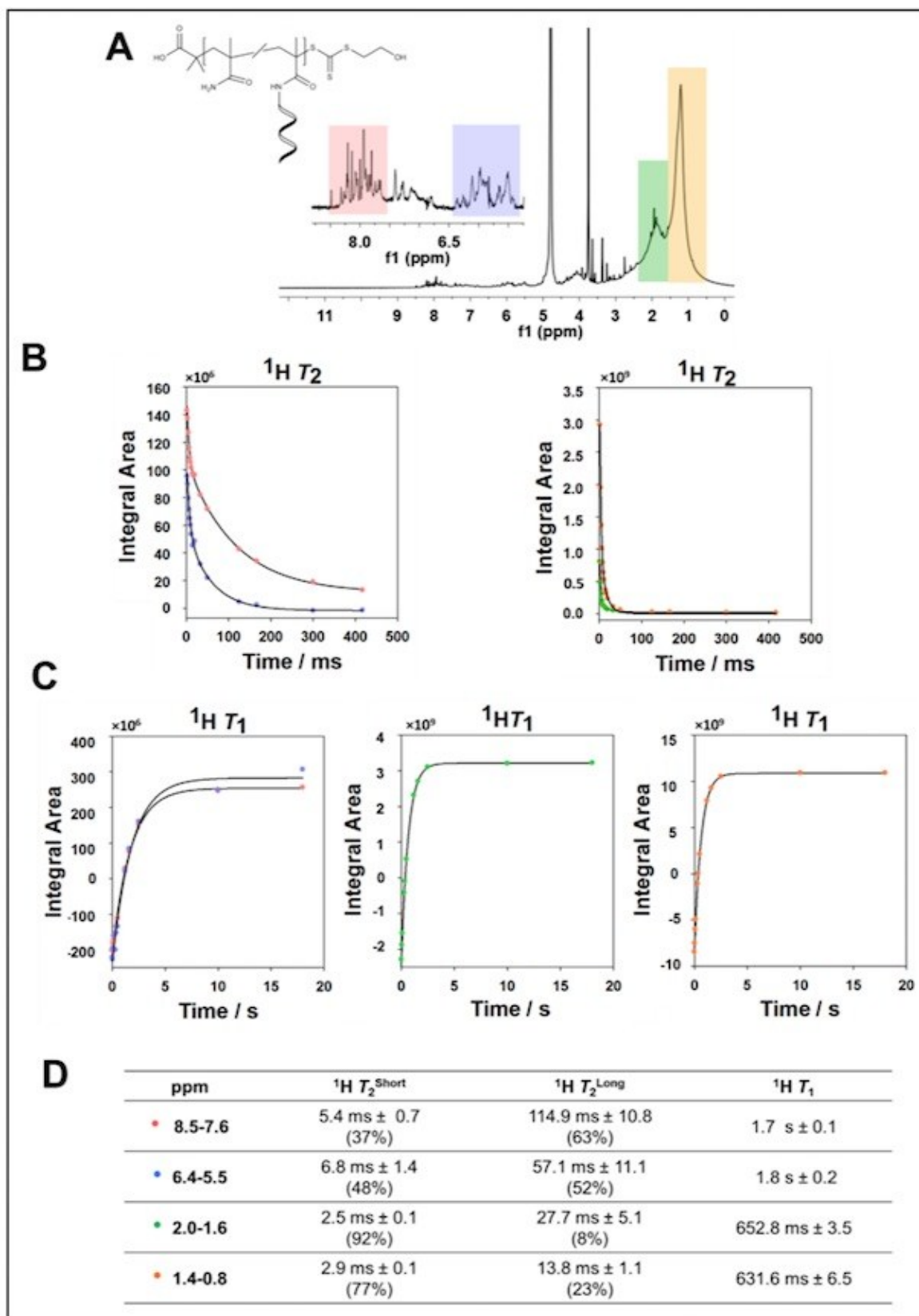


Fig. S11 (A) 1D ^1H NMR of p(MAm-c-MAmA1) in D_2O containing 50mM NaCl, 10mM Tris, 2mM EDTA pH 7.5. (B) $^1\text{H } T_2$ and (C) $^1\text{H } T_1$ relaxation measurements for protons resonating at 8.5-7.6 ppm (pink circles), 6.4-5.5 ppm (blue circles), 2-1.6ppm (green circles) and 1.4-0.8 ppm (orange circles). $^1\text{H } T_2$ s were fitted with biexponential decay curves. $^1\text{H } T_1$ s were fitted with single exponential decay curves. (D) List of $^1\text{H } T_2$ and $^1\text{H } T_1$ relaxation times with relative standard errors measured for proton resonating at 8.5-7.6 ppm, 6.4-5.5 ppm, 2-1.6 ppm and 1.4-0.8 ppm. The percentage of ^1H spins displaying short and long T_2 s is reported in brackets.

¹H diffusion analysis of p(MAm-c-MAmA1)

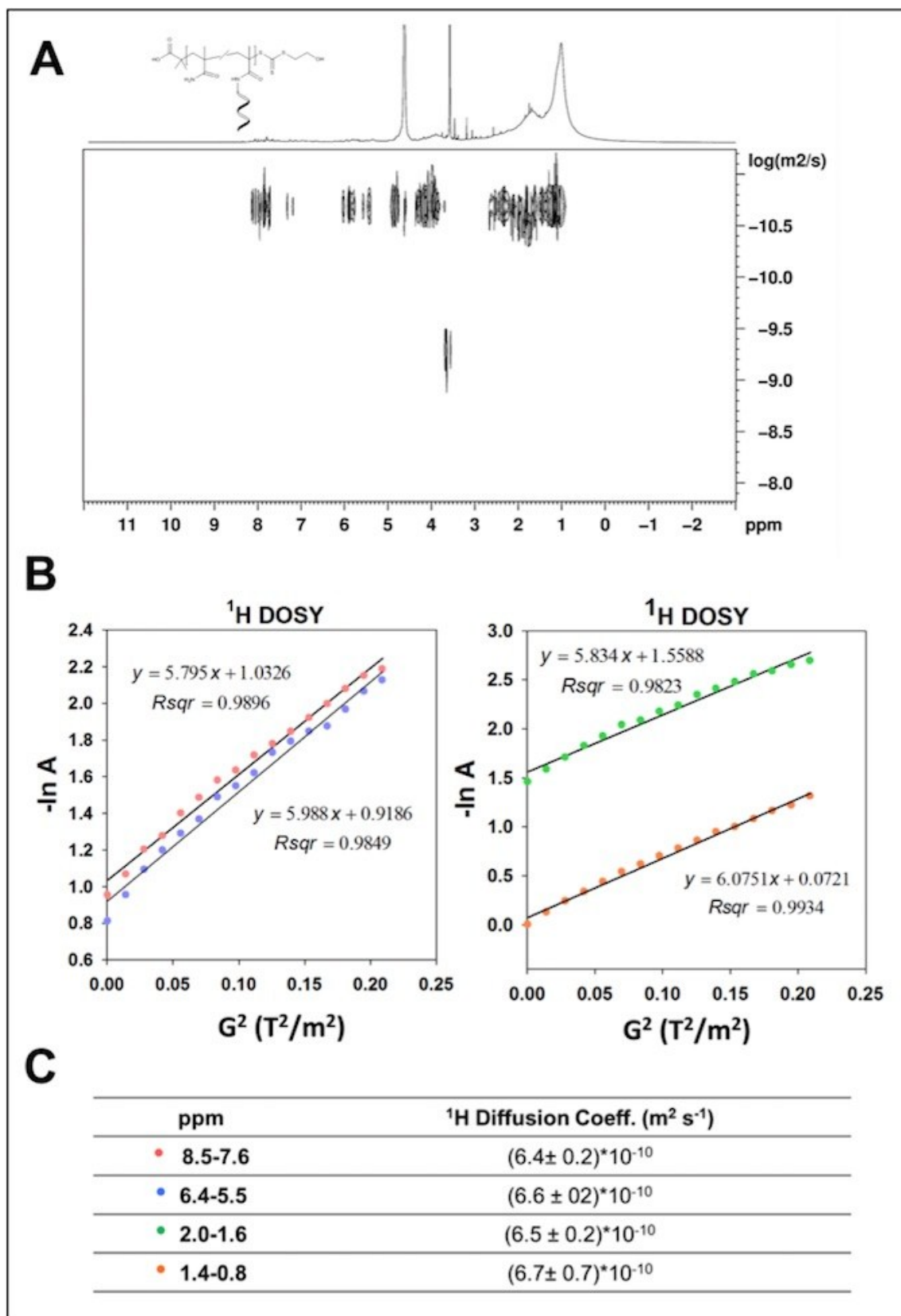


Fig. S12 (A) 2D ¹H DOSY spectrum of p(MAm-c-MAmA1). The regions selected for fitting analysis are highlighted in pink, blue, green and orange in the F2 projection. (B) The negative natural logarithm of the area of selected ¹H peaks at 8.5-7.6 ppm (pink circles), 6.4-5.7 ppm (blue circles), 2.0-1.6 ppm (green circles) and 1.4-0.8 ppm (orange circles) is plotted against the squared gradient strength. (C) List of ¹H self-diffusion coefficients measured for p(MAm-c-MAmA1) with their relative standard errors.

PAGE analysis of p(MAm-c-MAmA1B2)

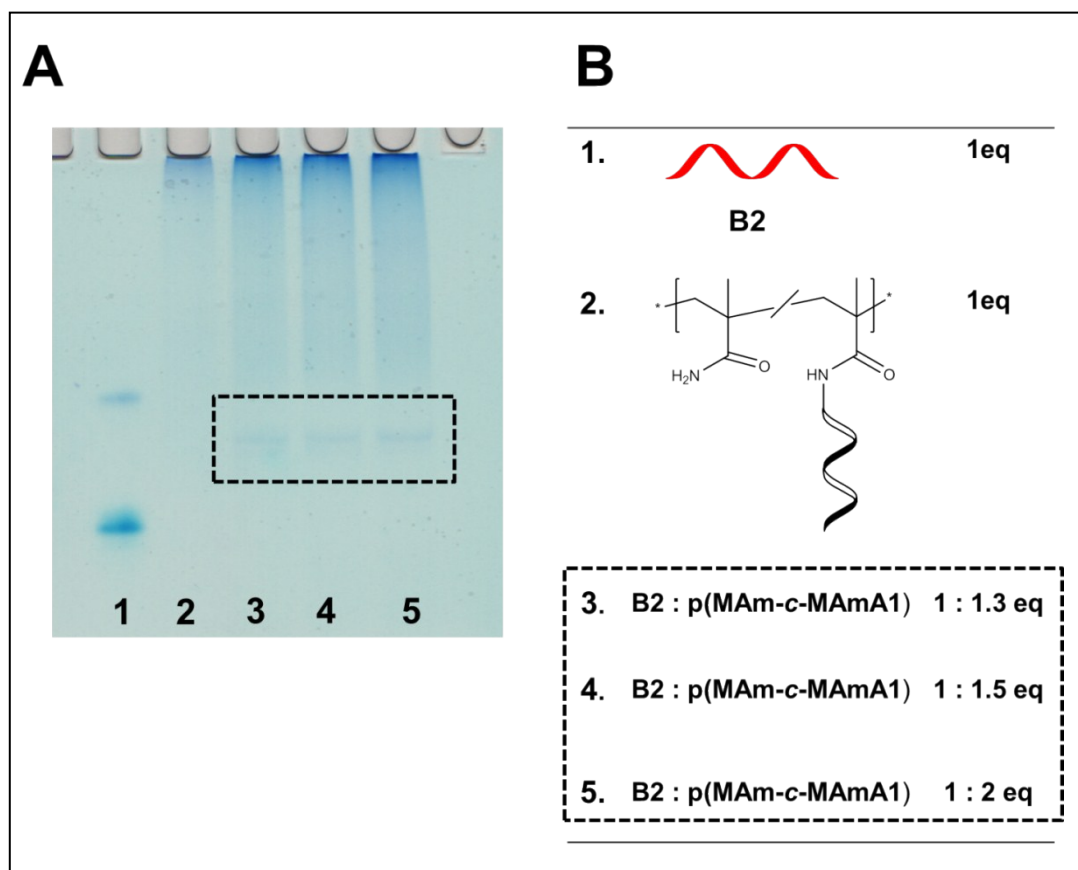


Fig. S13 (A) 20% native PAGE of B2 and p(MAm-c-MAmA1) annealed at different oligonucleotide molar ratios. Lanes: 1. B2, 2. p(MAm-c-MAmA1), 3. B2 : p(MAm-c-MAmA1) (1 : 1.3), 3. B2 : p(MAm-c-MAmA1) (1 : 1.5), 4. B2 : p(MAm-c-MAmA1) (1 : 2). (B) Schematic representation of the samples loaded in each lane of the 20% native PAGE. Highlighted area shows the presence of negligible traces of unbound strand B2 in all ratios screened.

^1H T_2 and T_1 relaxation of p(MAm-c-MAmA1B2)

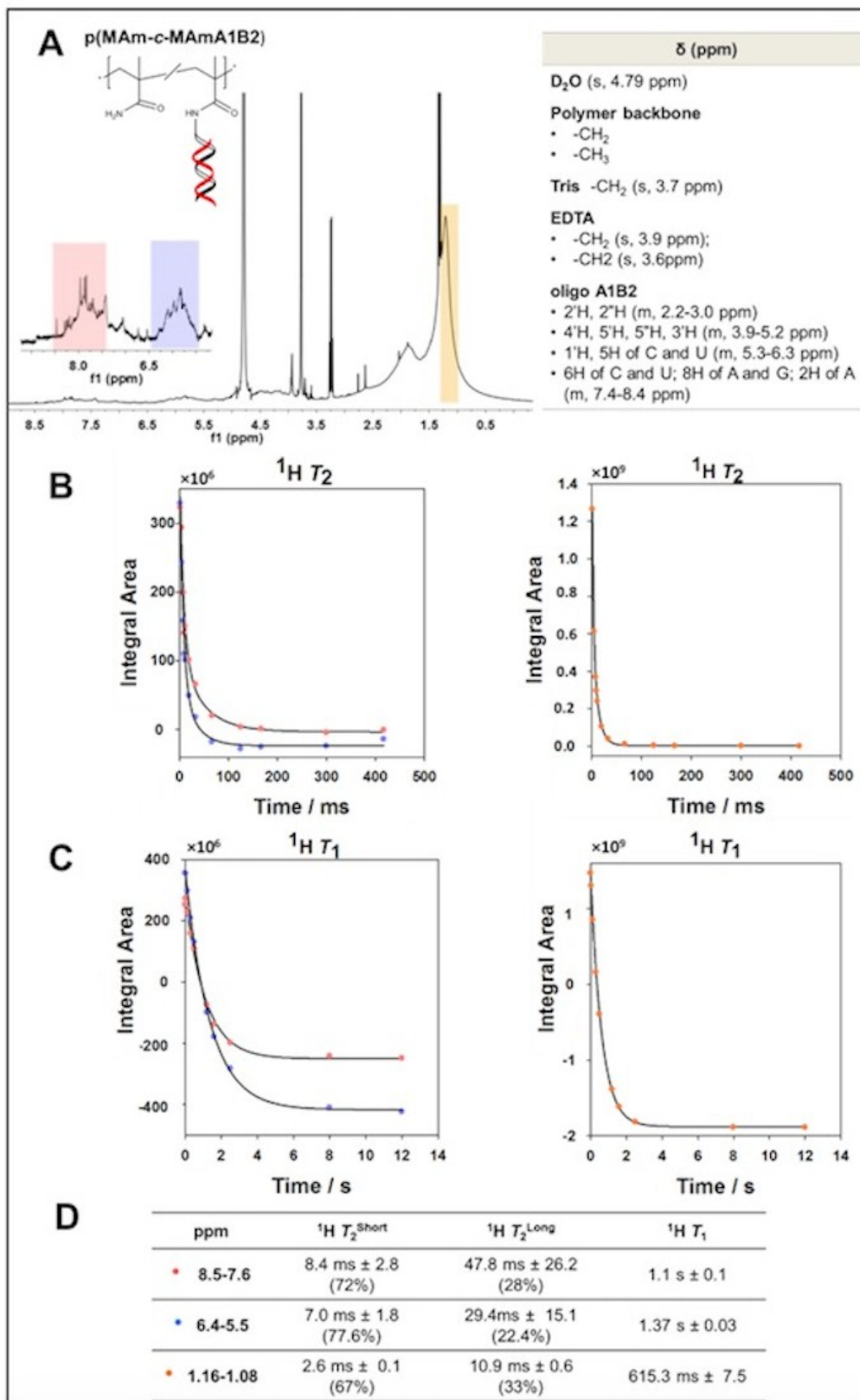


Fig. S14 (A) 1D ^1H NMR of p(MAm-c-MAmA1B2) in D₂O containing 50 mM NaCl, 10 mM Tris-HCl, 2 mM EDTA pH 7.5 with relative ^1H chemical shift assignments. (B) ^1H T_2 and (C) ^1H T_1 relaxation times measurements for ^1H resonating at 8.5-7.6 ppm (pink circles), 6.4-5.5 ppm (blue circles) and 1.16-1.08 ppm (orange circles). ^1H T_2 s were fitted with biexponential decay curves. ^1H T_1 s were fitted to single exponential decay curves. (D) List of ^1H T_2 s and ^1H T_1 s measured for p(MAm-c-MAmA1B2) with relative standard errors. The percentage of ^1H spins displaying short and long T_2 s is reported in brackets.

¹H diffusion analysis of p(MAm-c-MAmA1B2)

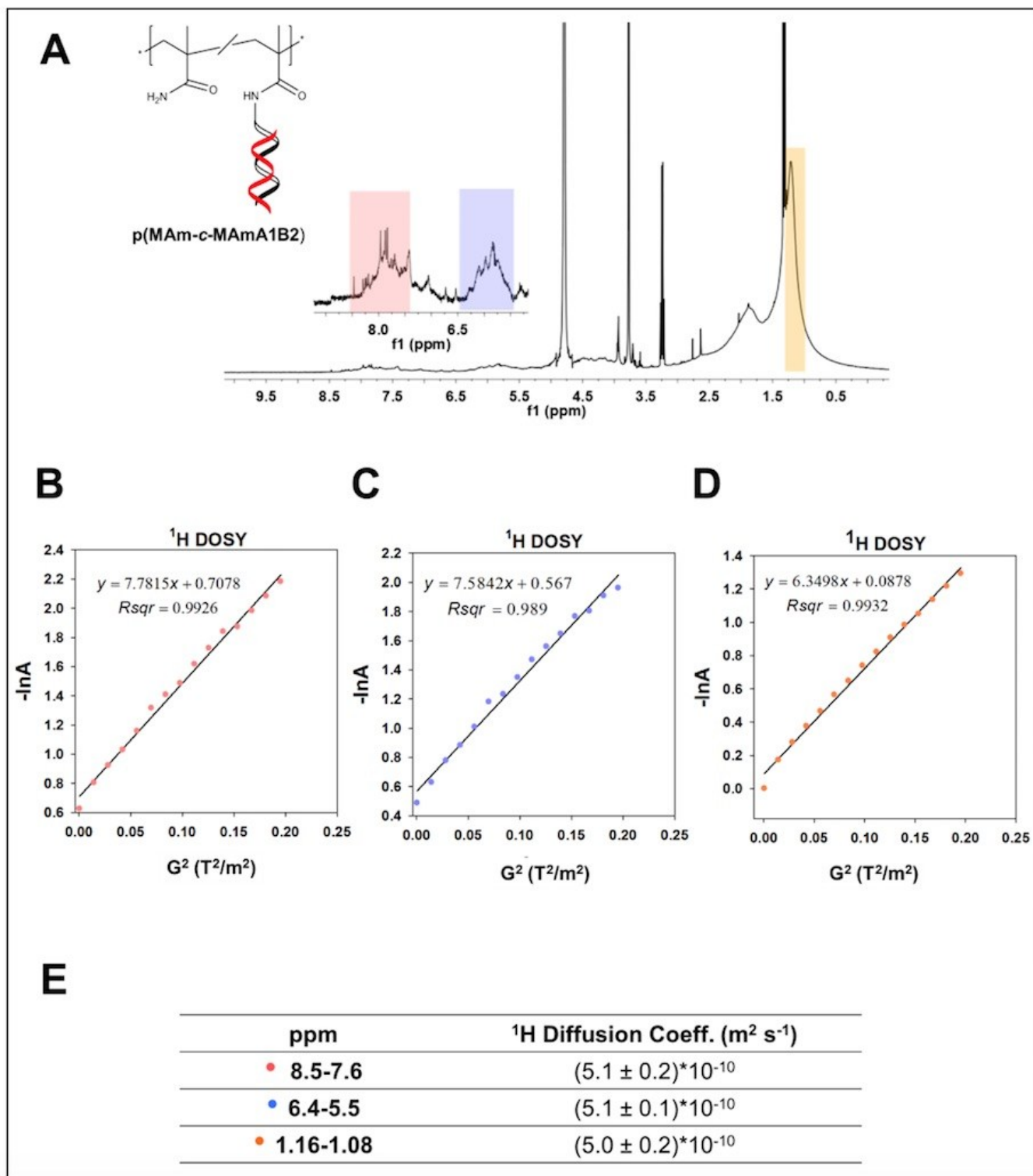


Fig. S15 (A) 1D ¹H NMR spectrum of p(MAm-c-MAmA1B2). The regions selected for fitting analysis are highlighted in pink, blue and orange in the F2 projection (B)-(D) The negative natural logarithm of the area of selected ¹H peaks at 8.5-7.6 ppm (pink circles), 6.4-5.5 ppm (blue circles) and 1.16-1.08 ppm (orange circles) is plotted against the squared gradient strength. (E) List of ¹H self-diffusion coefficients measured for p(MAm-c-MAmA1B2) with their relative standard errors.

¹⁹F diffusion analysis of B2, p(MAm-c-MAmA1B2) and p(MAm-c-MAmA1B2)+C

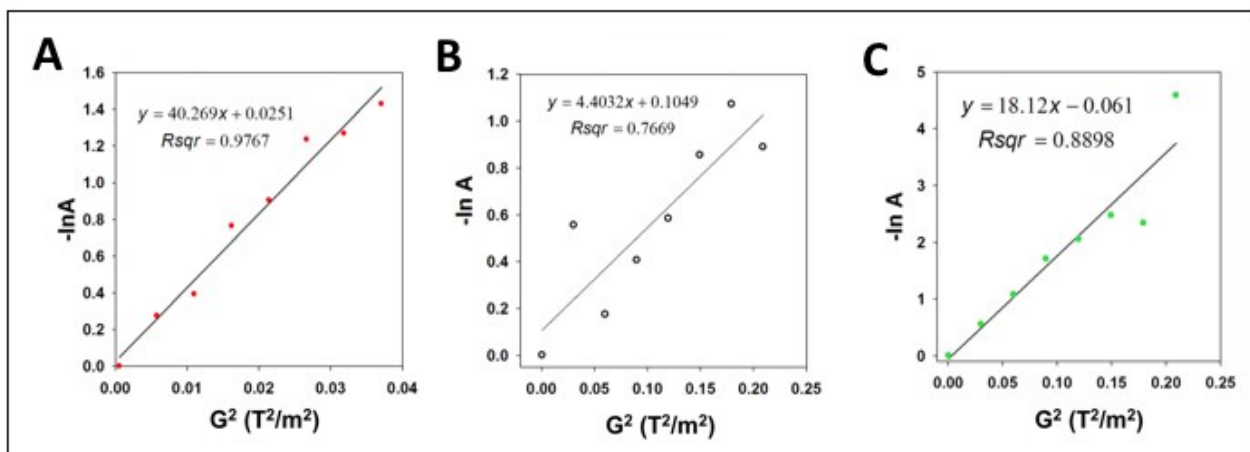


Fig. S16 The negative logarithm of the area of the ¹⁹F signal detected for (A) oligonucleotide B2, (B) p(MAm-c-MAmA1B2) and (C) p(MAm-c-MAmA1B2)+C is plotted against the squared gradient strength.

PAGE analysis of p(MAm-c-MAmA1B2)C

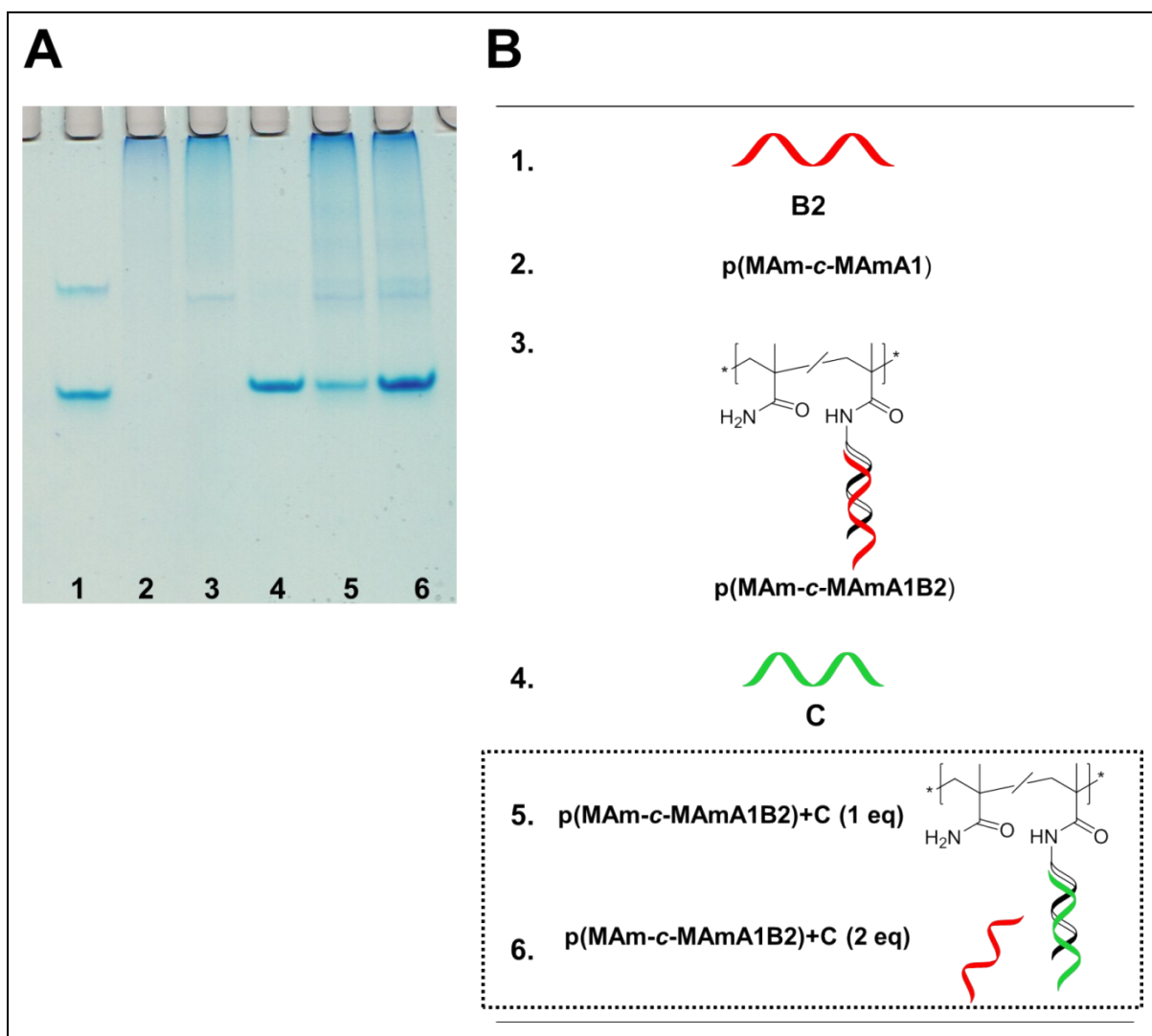


Fig. S17 (A) 30% native PAGE testing the strand displacement process in presence of the target DNA strand C. Lanes: 1. B2, 2. p(MAm-c-MAmA1), 3. p(MAm-c-MAmA1B2) (1:1.3), 4. C, 5. p(MAm-c-MAmA1B2)C (1:1.3:1), 6. p(MAm-c-MAmA1B2)C (1:1.3:2). (B) Schematic representation of the samples loaded in each lane of the 30% native PAGE.

^1H T_2 and T_1 relaxation of p(MAm-c-MAmA1B2)C

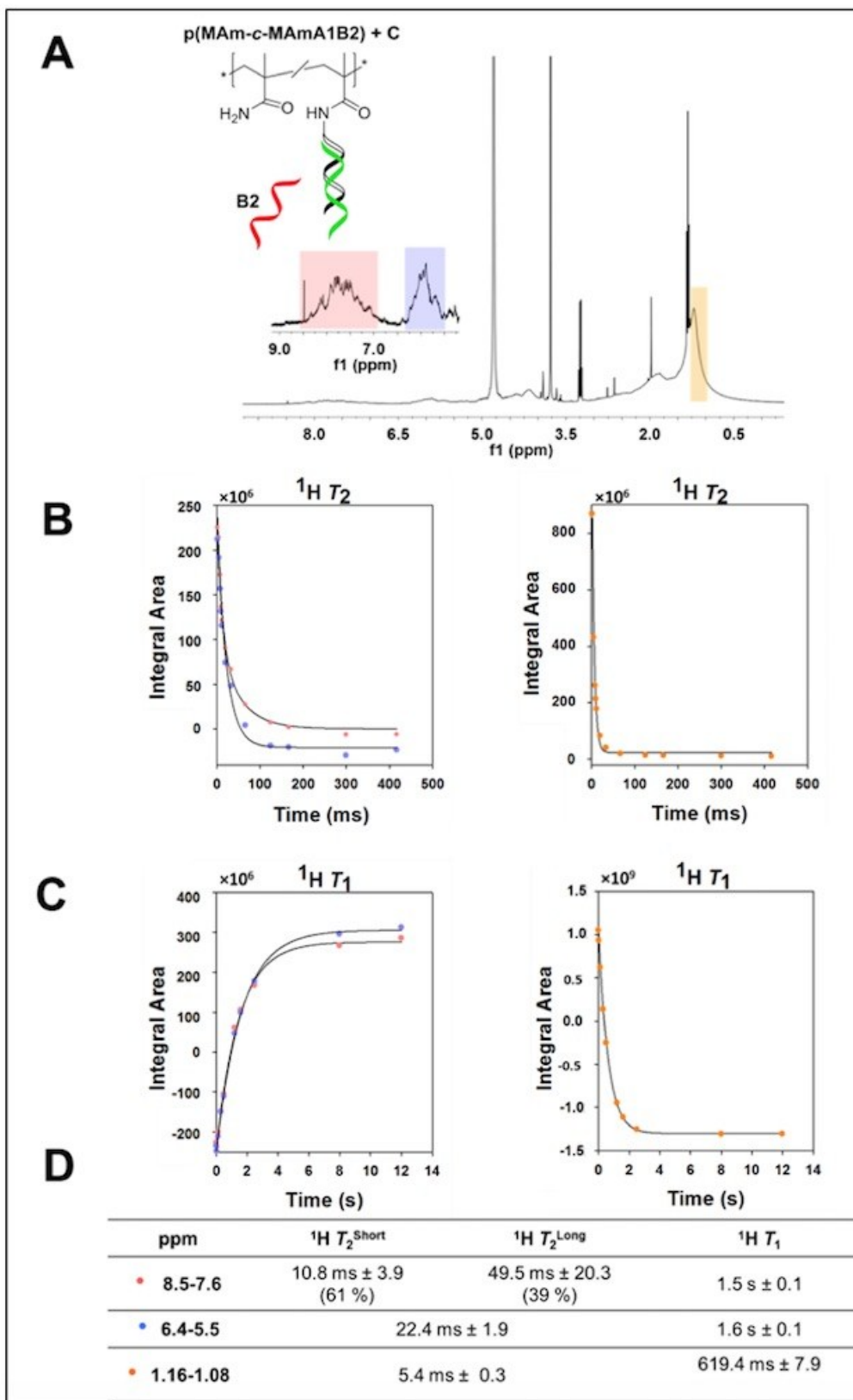


Fig. S18 (A) 1D ^1H NMR with relative chemical shift assignments of p(MAm-c-MAmA1B2) after 30 min from the incubation with 1 molar equivalent of strand C. (B) ^1H T_2 and (C) ^1H T_1 relaxation times measurements for ^1H resonating at 8.3-7.2 ppm (pink circles), 6.2-5.4 ppm (blue circles) and 1.16-1.08 ppm (orange circles). ^1H T_2 s were fitted with biexponential decay curves. ^1H T_1 s were fitted to single exponential decay curves. (D) List of ^1H T_2 s and ^1H T_1 s measured for p(MAm-c-MAmA1B2)C with relative standard errors. The percentage of ^1H spins displaying short and long T_2 s is reported in brackets.

^1H diffusion analysis of p(MAm-c-MAmA1B2)C

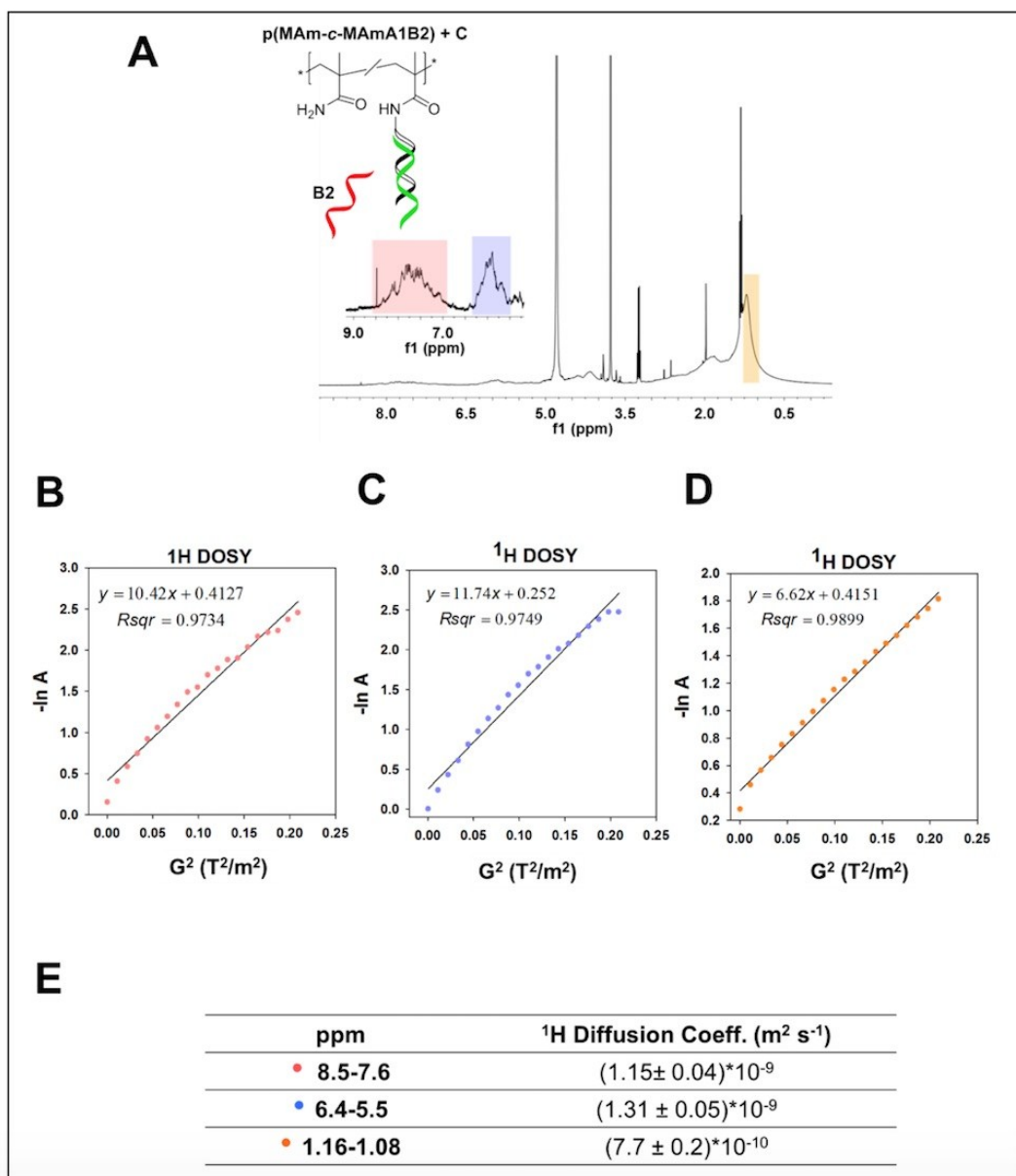


Fig. S19 (A) 1D ^1H NMR spectrum of p(MAm-c-MAmA1B2) incubated with 1 molar equivalent of strand C. The regions selected for fitting analysis are highlighted in pink, blue and orange in the F2 projection. (B)–(D) The negative natural logarithm of the area of selected ^1H peaks at 8.3–7.2 ppm (pink circles), 6.2–5.4 ppm (blue circles) and 1.16–1.08 ppm (orange circles) is plotted against the squared gradient strength. (E) List of ^1H self-diffusion coefficients measured for p(MAm-c-MAmA1B2)C with their relative standard errors.

1. K. Levenberg, *Quarterly Journal of Applied Mathematics*, 1944, II, 164-168.
2. D. H. Wu, A. D. Chen and C. S. Johnson, *Journal of Magnetic Resonance, Series A*, 1995, 115, 260-264.